

Numerical and Experimental Studies of Mixing of High Temperature Critical Water

Khokhar ZHI, Al-Harhi MA

Department of Chemical Engineering, King Fahad University of Petroleum & Minerals, Dhahran, Saudi Arabia

email: zahedhk@gmail.com, mamdouh@kfupm.edu.sa, phone +966-3-860-7797, Fax: +966-3-860-4234

Abstract— In specialty chemical industry, nano-sized materials exhibit a key role. Their synthesis routes involve noxious chemicals as well as expensive precursors. Super critical water offers a relatively simple route which is inherently scaleable and chemically benign. In this work, experimental observations of a high pressure optical cell are simulated and these preliminary results are compared with mixing at room temperature. Opposed-tee geometries are constructed and investigated for high temperature water mixing. Convective flow strongly influenced the mixing pattern was observed simulating the runs using CFD package. Mixing direction also affects the flow pattern. Further modifications are proposed in the design on the basis of these results.

I. INTRODUCTION

A supercritical fluid possesses the characteristics of both fluid and gaseous substances: the fluid behavior of dissolving soluble materials, and the gaseous behavior of excellent diffuse ability. In the case of supercritical water particularly, the effect as a reaction-causing solvent is great. The physical properties such as density, permittivity, and ion product can be widely controlled by temperature and pressure. Many organic and inorganic syntheses were carried out using super critical water as reaction media. Synthesis of fine chemicals such as mono terpene alcohols [1] as well as commodity chemicals such as ϵ -caprolactam [2] in supercritical water has been done. Super-critical water was also investigated as electrolytic solvent [3]. Its environment is also used to study corrosion properties of oxide dispersion strengthened steels [4], hydrolysis and oxidative decomposition of ethyl acetate [5] and reactions of model compounds of phenol resin [6]. Few other discussions are available about chemical synthesis and reactions at super critical conditions [7-9]. Metal oxide nano wires and nano particles were produced by using supercritical water [10, 11]. Continuous hydrothermal synthesis of inorganic materials in a near-critical water flow reactor has been investigated [12].

In present studied system, reactant stream at room temperature and at system pressure is mixed with a high-temperature water stream at the system pressure to achieve rapid heating of solutions to supercritical conditions. These reactions are extremely fast and the process is done efficiently. Simulations of mass and heat transfer are necessary to design super critical water processes. Computational fluid dynamics (CFD) packages can provide

some insight into the engineering aspects of the reacting and flowing mixtures as experimental verification. The mixing phenomena between high temperature water and room temperature water seems to be unique among technological methods and results in an abrupt variation of physical and transport properties with changes in temperature or pressure. The mixing phenomenon is important in the rapid heating of reactants or possibly to suppress side reactions to suppress crystal growth. Based on construction of optical cells for supercritical carbon dioxide [13] and supercritical water [14] a mixing observation cell for channel-tee type mixing was designed and the preliminary results [15] are investigated in this study with further modifications [16]. These modifications can be used to improve the simulations and pseudo-supercritical water mixing [17, 18] and to better understand the phenomenon for different geometries. The main interest of this work concentrates around the opposed tee and the side tee shown in Figure 1 and further modification to these designs.

II. MODEL EQUATIONS

The differential equations representing the conservation equations (mass, momentum and energy) can be written in a general form:

$$\frac{\delta(R_i \rho_i \phi_i)}{\delta t} + \text{div} \left(R_i \rho_i U_i \phi_i - R_i \Gamma_{\phi_i} \text{grad} \phi_i \right) = R_i S_i \quad (\text{A})$$

transient convection diffusion source

where ϕ_i is any conserved property of phase i , Γ_{ϕ_i} is exchange coefficient of ϕ in phase i , R_i is volume fraction of phase i , S_{ϕ_i} is source rate of ϕ_i , and U_i is velocity vector of phase i

Thus, the continuity equation, e.g., for phase i become:

$$\text{div}(R_i \rho_i U_i) + \frac{\partial(R_i \rho_i)}{\partial t} = m_i \quad (\text{B})$$

where m_i is mass per unit volume entering phase i from all sources, ρ_i density of phase i , D_i is diffusivity of phase i , and the conservation of momentum for variable ϕ_i becomes:

$$\text{div} \left(R_i \rho_i U_i \phi_i - R_i \mu_{\text{eff}} \text{grad} \phi_i \right) = R_i S_{\phi_i} \quad (\text{C})$$

where μ_{eff} is effective viscosity, and S_{ϕ_i} is Source of ϕ_i per unit volume. Similarly, the equation of energy can be written.

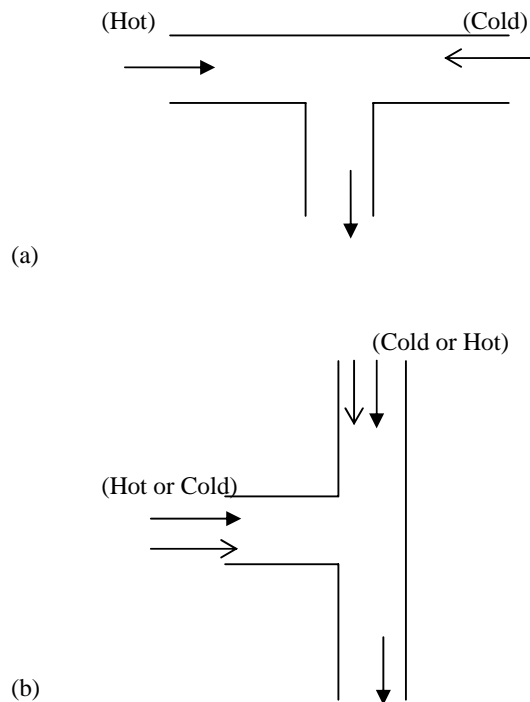


Fig. 1: Experimental Geometry Designs used for Simulations

III. EXPERIMENTAL WORK

A complete visualization of the mixing point at high-temperature and high pressure conditions were set up by dividing one-piece window to three parts in function to avoid strain and catastrophic failure to get safer design. Experiments were done for different tee geometries as shown in Fig. 1. Observations were done using a diffuse white-light source [14] whereas for low temperatures, thermocouples were used [15].

In Fig. 1a high temperature water was introduced from left side of the tee and a dye mixed room temperature water was introduced from right (opposite) side whereas mixed fluid was flown out from downside of the tee. Fig. 1b was used in two ways. Firstly, the high temperature water was introduced from top and the dye mixed room temperature water was introduced from left side whereas product stream was flown out from bottom. Secondly, the high temperature water was introduced from left side and the dye mixed room temperature water was introduced from top whereas product stream was flown out from bottom. Mixing at high temperature water at 389.16, 507.16, 620.16, and 711.16K at 6526.7 *psi* was observed for flow rate ratio between high temperature water and room temperature water of 5:1 ($1.7657 \times 10^{-5} \text{ ft}^3/\text{min}$: $3.5315 \times 10^{-6} \text{ ft}^3/\text{min}$). Final solution temperatures were 373.16, 473.16, 573.16, and 673.16K,

respectively. These precise temperature values were determined by calculation using an energy balance. Experimentally, the cell wall was heated to 373.16, 473.16, 573.16, and 673.16K, respectively to compensate the heat losses and matching the outlet temperature of mixed stream which is not the case in simulation geometries. In super critical water, it is not clear that classical approaches to flow regimes, such as Reynolds number, are strictly valid, however, it is assumed that the fluid was homogeneous by the perfect mixing. These after complete mixing were 5-70 under such conditions expecting a laminar flow [14].

IV. NUMERICAL MODEL

Experimentally, decomposition of dye was a concern at higher temperatures, which is not the case in simulation work. Temperature gradient is coloured by the CFD package after convergence of simulation runs and is solely a matter of presenting results.

Mass and momentum conservation equations were solved. The energy equation was enabled during simulations and flow pattern were observed using temperature fields. The general purpose three-dimensional CFD package FLUENT was used to solve the governing equations. A three-dimensional numerical model representing as Fig 1 was constructed of width 0.0787 *in* and of depth 0.0984 *in* using pre-processor Gambit. An unstructured tetrahedral grid was chosen. It has already been investigated that during simulation no significant effect is observed due to upstream and down stream lengths in simulations [15]. $k-\epsilon$ turbulence model was used for simulation work. Fig. 2 shows good agreement between experiments and simulation results of numerical model used for investigations. It is then applied for further study cases. The mesh size has to be small enough in order to resolve properly the fields that are solved for. Using mesh size of 0.003 937 *in*, 299 920 and 300 033 tetrahedral cells were used for Fig. 1a and 1b geometries, respectively. Boundary conditions are different for each case.

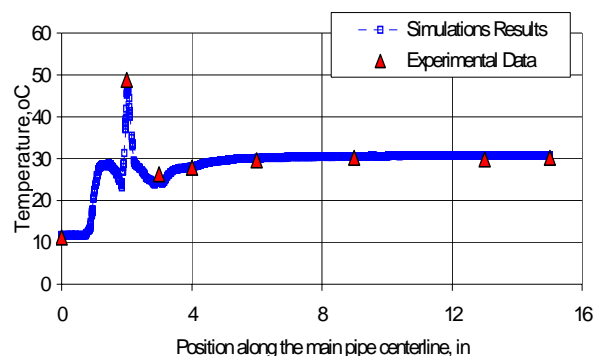


Figure 2: Comparison of numerical results with experimental observations.

V. RESULTS AND DISCUSSION

Results of the mixing of opposed side tee are shown in Figure 3. High temperature water entered from the left side of tee whereas room temperature water flowed in from the right side (Fig. 1a). The outlet of the tee is at the bottom.

Flow rate differences makes mixing more convenient whereas equal flow rates from opposite sides delay the mixing. This kind of equal opposite flow rate mixing delay is shown in Figure 2 for high velocities for flow rate ratio between high temperature water from bottom to room temperature water from top 1.07:1.0.

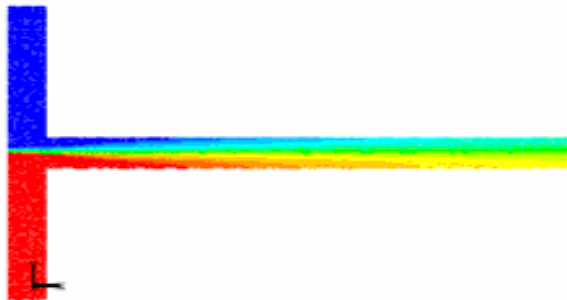


Fig. 3: Opposed-flow making delay in mixing for flow rate ratio between high temperature water and room temperature water 1.07: 1.0.

To avoid this kind of mixing behaviour higher flow rate ratios are used. The cases which are simulated and results are shown in Fig. 4 has a ratio of 5:1 between high temperature water and room temperature water. Flow rate of high temperature water is $1.7657 \times 10^{-5} \text{ ft}^3/\text{min}$ and that of room temperature water is $3.5315 \times 10^{-6} \text{ ft}^3/\text{min}$.

A good agreement is found between flow patterns of experimental work [14] and our simulated work using CFD package Fluent 6.0. Fig. 4 shows that for this case high temperature water flowed above the room temperature water at the point of mixing due to density differences between the two streams. This phenomenon also signifies the gravity effects on flow. Temperature field is also moving towards right at mixing point showing the effect of high temperature stream convections to room temperature water stream for low high temperature water to higher high temperature water (Fig. 4a-d).

Thermal and transport properties of mixing streams became more apparent with back mixing phenomenon and turbulence region formation when Fig. 1b geometry was used to mix the high temperature water with room temperature water. High temperature water and room temperature water was introduced alternatively from left side and from top side whereas the mixed stream outlet was at bottom. This geometry was also designed and constructed. Simulation runs done for the different cases are shown in Fig. 5 for this geometry. High temperature water at 769.16 K entered from the side and room temperature water at room temperature flowed in from the top. It can be seen from the Fig. 5a that temperature contours are

distinguishing temperature fields for high temperature to room temperature.

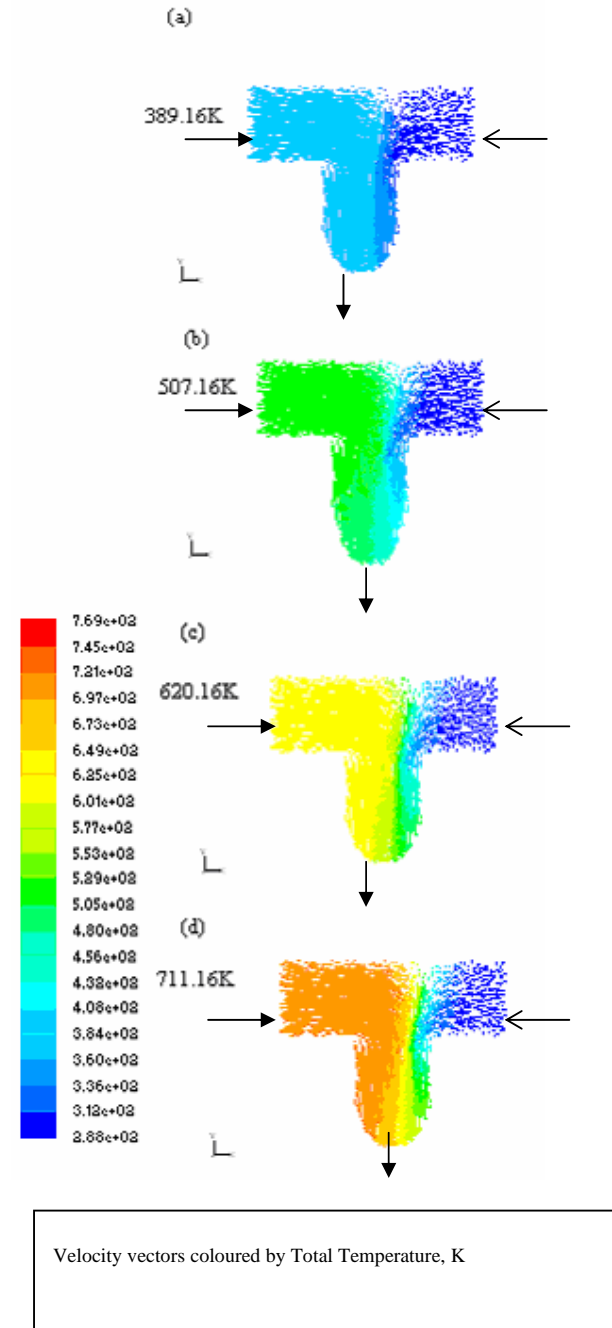


Fig. 4: Simulation results of mixing various temperatures at 6526.7 psi. Flow rates of high temperature water and room temperature water are $1.7657 \times 10^{-5} \text{ ft}^3/\text{min}$ $3.5315 \times 10^{-6} \text{ ft}^3/\text{min}$, respectively. High temperature water comes from left side, and room temperature water comes from right side. Temperature of high temperature water is (a) 389.16K, (b) 507.16K, (c) 620.16K, and (d) 711.16K, respectively.

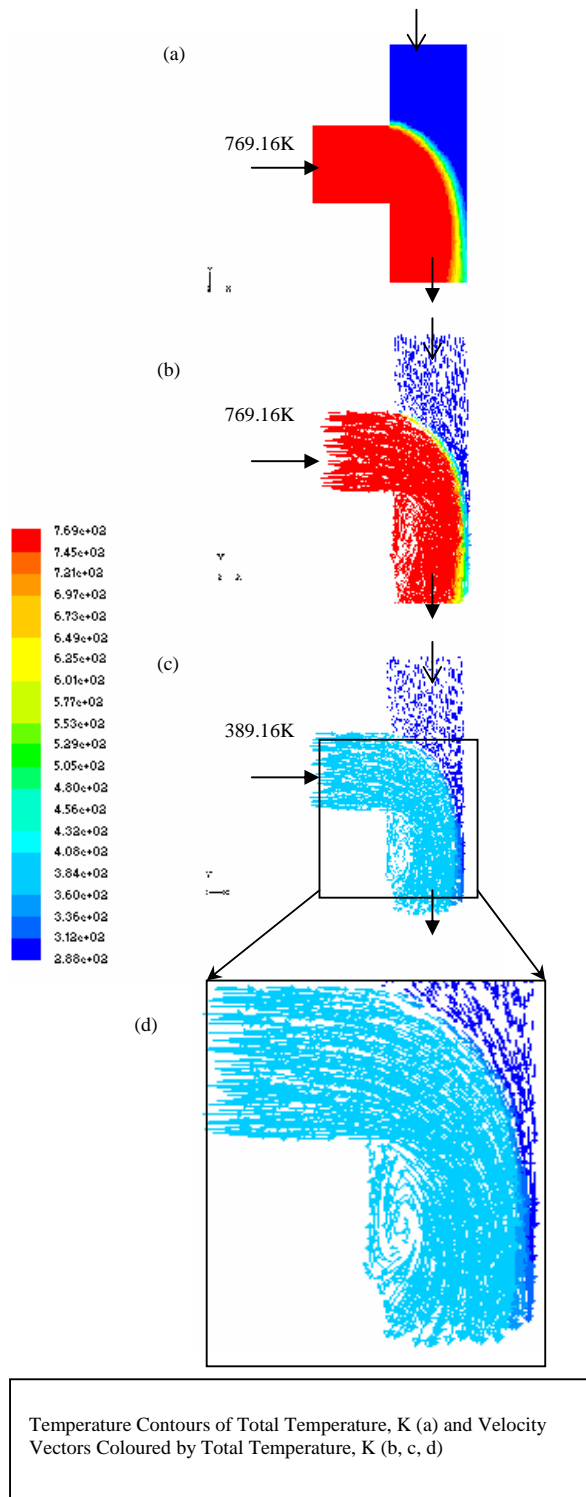


Fig. 5: Simulation results of mixing various temperatures at 6526.7 psi. Flow rates of high temperature water and room temperature water are $1.7657 \times 10^{-5} \text{ ft}^3/\text{min}$ $3.5315 \times 10^{-6} \text{ ft}^3/\text{min}$, respectively. High temperature water comes from left side, and room temperature water comes from top side. Temperature of high temperature water is (a) 769.16K, (b) 769.16K, (c) 389.16K, and (d) magnified case (c) to observe back-mixing and swirling flow, respectively.

A significant temperature penetration region can be seen increasing and expanding with downward flow and moving away from the centre towards the opposite wall of the high temperature water inlet. For higher high temperature water case (Fig. 4a, b) this temperature mixing region is significant than for low high temperature water case (Fig. 4c). During experimenting, scale does not change for direct eye or camera observations for different cases. However, CFD post processing can handle the same case for different scales and becomes a powerful media to observe the inside phenomenon more deeply and clearly.

Velocity vectors coloured with total temperature show turbulent flow with many multitudes of eddies occurring. Formation of turbulent back-mixing region can be seen for this case. Reynolds number was estimated to 70 after complete mixing, which is in laminar flow region. Fig. 4d shows that the high temperature water flows into and above the room temperature water engulfing it and makes a whirl pattern. This engulfing phenomenon can be used to modify the geometry and enhancing the possibilities to allow high temperature water mixing into room temperature water.

Some of these modifications are mentioned later in this study. In summary, mixing at high temperature high-pressure conditions is simulated and simulation results are found in good agreement at observation level. All results presented are for mixing in the laminar flow region. More cases may be simulated for these geometries.

Convective flow strongly influenced the mixing pattern. Keeping in view this point, many modifications may be proposed in designing the geometries for opposed flow mixing. Some are shown in Fig. 6.

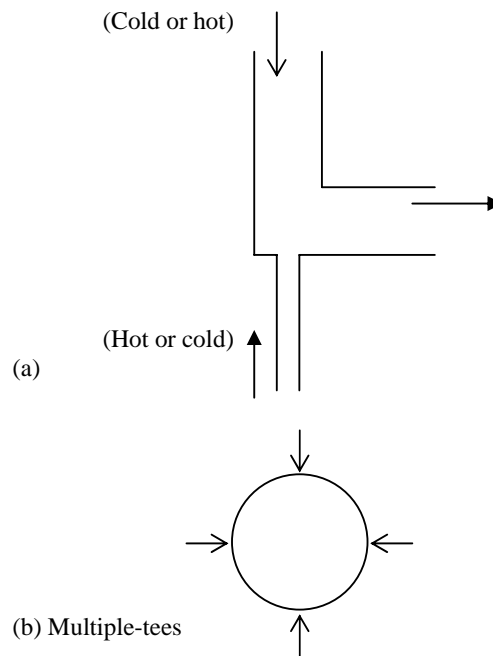


Figure 6: Modification proposed in Geometry Designs (a) An engulfed opposed tee (b) Multiple-tees

In Fig. 6a which is a modification of Fig. 1, high temperature water enters from top and room temperature water flows in from bottom or alternatively. Very early mixing can be observed in this case due to back mixing, swirl flow, engulfing and convections taking place in small area. These phenomena may be explored using multiple tees considering high temperature critical water mixing (Fig. 6b).

VI. CONCLUSIONS

Convective flow strongly influenced the mixing pattern which should be considered whenever mixing geometries are designed. These results possibly will be applicable to many current material synthesis schemes and also for micro-reactor design for high temperature super-critical fluids for research and development purposes.

ACKNOWLEDGMENT

The authors would like to acknowledge the support of KFUPM during the course of this work.

REFERENCES

- [1] Y. Ikushima, M. Sato, A one-step production of fine chemicals using supercritical water: an environmental benign application to the synthesis of monoterpene alcohol, *Chem. Eng. Sci.* 59 (2004) 4895–4901.
- [2] Y. Ikushima, O. Sato, M. Sato, K. Hatakeda, M. Arai, Innovations in chemical reaction processes using supercritical water: an environmental application to the production of ϵ -caprolactam, *Chem. Eng. Sci.* 58 (2003) 935–941.
- [3] E. Franck, Super-critical water as electrolytic solvent. *Angew. Chem.* (1961), 73 309-22.
- [4] H. Cho, A. Kimura, S. Ukai, M. Fujiwara, Corrosion properties of oxide dispersion strengthened steels in super-critical water environment. *Journal of Nuclear Materials* (2004), 329-333(Pt. A), 387-391.
- [5] U. Armbruster, A. Martin, A. Krepel, Hydrolysis and oxidative decomposition of ethyl acetate in sub- and super-critical water. *Applied Catalysis, B: Environmental* (2001), 31(4), 263-273.
- [6] H. Tagaya; K. Katoh; M. Karasu; J. Kadokawa; K. Chiba, Reactions of model compounds of phenol resin in sub- and super-critical water. *Preprints of Symposia - A C S, Division of Fuel Chemistry* (1999), 44(2), 354-356.
- [7] R. van Eldik, T. Asano, W.J. le Noble, Activation and reaction volumes in solution. 2, *Chem. Rev.* 89 (1989) 549–688.
- [8] P. Savage, S. Gopalan, T. Mizan, C. Martino, E. Brock, Reactions at supercritical conditions—applications and fundamentals, *AIChE J.* 41 (1995) 1723–1778.
- [9] P. Jessop, W. Leitner, *Chemical Synthesis Using Supercritical Fluids*, Wiley/VCH, Weinheim, 1999.
- [10] T. Adschiri, Y. Hakuta, K. Arai, Hydrothermal synthesis of metal oxide fine particles at supercritical conditions, *Ind. Eng. Chem. Res.* 39 (2000) 4901–4907.
- [11] Y. Hakuta, H. Hayashi, K. Arai, Hydrothermal synthesis of photocatalyst potassium hexatitanate nanowires under supercritical conditions, *J. Mater. Sci.* 39 (2004) 4977.
- [12] A. Cabanas, A. Darr, E. Lester, M. Poliakoff, Continuous hydrothermal synthesis of inorganic materials in a near-critical water flow reactor; the one-step synthesis of nano-particulate $Ce_{1-x}Zr_xO_2$ ($x=0-1$) solid solutions, *Journal of material chemistry*, 11 (2001) 561-568
- [13] T. Aizawa, M. Kanakubo, Y. Ikushima, N. Saitoh, K. Arai, R.L. Smith Jr., “Totsu”-window optical cell for absorption and emission studies of high-pressure liquids and supercritical fluids, *J. Supercrit. Fluids* 29 (2004) 313–317.
- [14] T. Aizawa, M. Kanakubo, Y. Ikushima, R.L. Smith Jr., T. Saitoh, N. Sugimoto, Local density augmentation around acetophenone N,N,N',N' -tetramethylbenzidine exciplex in supercritical water, *Chem. Phys. Lett.* 393 (2004) 31–35.
- [15] T. Aizawa, Y. Masuda, K. Minami, M. Kanakubo H. Nanjo, R.L. Smith, Direct observation of channel-tee mixing of high-temperature and high-pressure water, *J. Supercrit. Fluids* 43 (2007) 222–227.
- [16] Z. Khokhar, Investigation of mixing in pipe with side-, opposed-, and multiple-tees, M.Sc. Thesis, KFUPM, Dhahran, Saudi Arabia, Dec. 2002
- [17] P. Blood, J. Denyer, B. Azzopardi, M. Poliakoff, E. Lester, A versatile flow visualisation technique for quantifying mixing in a binary system: application to continuous supercritical water hydrothermal synthesis (SWHS), *Chem. Eng. Sci.* 59 (2004) 2853–2861.
- [18] E. Lester, P. Blood, J. Denyer, D. Giddings, B. Azzopardi, M. Poliakoff, Reaction engineering: the supercritical water hydrothermal synthesis of nano-particles, *J. Supercrit. Fluids* 37 (2006) 209–214.